THE ASTROPHYSICAL JOURNAL, 231:128–138, 1979 July 1

THE CIRCUMSTELLAR ENVELOPES OF M GIANTS

ANN MERCHANT BOESGAARD
Institute for Astronomy, University of Hawaii
AND
WENDY HAGEN*
Harvard-Smithsonian Center for Astrophysics
Received 1978 November 9; accepted 1979 January 11

ABSTRACT

High-dispersion (5–10 Å mm^{-1}) spectra have been used to investigate the properties of the circumstellar (CS) envelopes of 61 M III stars with M_v fainter than -2.5 as they vary with spectral class. Observations of the velocities, equivalent widths, and line profiles of circumstellar Ca II K4, Hα, and the Na I D lines are presented. The CS Ca II lines increase in strength while the velocity centroid decreases as the long wavelength edge moves toward the red. The shells are modeled as extended, expanding envelopes. Comparison of calculated and observed line profiles shows that the K4 lines are formed over an increasing velocity gradient and that the turbulence in the shell increases from ≤ 2 km s^{-1} for M0 giants to ≥ 4 km s^{-1} for M6 giants. The strength of the Ca II K4 feature is much more sensitive to turbulence and velocity gradients than to optical depth; mass-loss rates based on these lines are therefore not reliable. Circumstellar components of the Na I D lines appear for giants of type M2 and cooler and show only marginal increases in strength and velocity for cooler stars. These lines give Doppler velocities of $\sim$3–4 km s^{-1} for the middle and late M giants. An asymmetry at Hα is visible in about 50% of the stars of all spectral types. This indicates that expansion occurs within the chromospheric regions, which in turn implies that the mechanism of mass loss is probably not radiation pressure on grains. Since no CS Ca II is seen at the stellar velocity in the earlier M stars, either the mass-loss mechanism must accelerate extremely rapidly to a terminal velocity or act upon Ca III which then recombines to Ca II after the terminal velocity has been reached. The supersonic stellar winds discussed by Mullan may drive the mass loss.

Subject headings: stars: circumstellar shells — stars: late-type — stars: mass loss

I. INTRODUCTION

Circumstellar (CS) envelopes of and mass loss from late-type giants and supergiants have been observed through violet-displaced absorption cores in strong, low-excitation lines, the 10 μm silicate dust feature, and/or molecular masering at radio wavelengths. The strength of the CS features appears to increase toward later spectral type and with increasing luminosity. Because of the greater number of giants and their greater homogeneity as a group compared to supergiants, study of the CS envelopes of the luminosity class III stars is a useful way to investigate the dependence of the properties of the envelopes on spectral class. The first survey of the CS envelopes of M giants was by Deutsch (1960), who found that the strong CS absorption features of Ca II H and K (herein referred to as H4 and K4 to distinguish them from the chromospheric absorption H3 and K3) were seen for all M giants later than M0 and increased in strength toward later types because of a widening of the feature. The sharp blue edge of the profile remained at roughly the same position, while the red edge moved redward, resulting in a wider line with the center of gravity (the measured line velocity) less blue-shifted. Deutsch suggested that the weakening of lines with earlier spectral type could be due to either a decrease in the amount of matter in the shell, or an increasing ionization from the observable Ca II to Ca III. He suggested that the expansion velocity increases outward through the shell to a terminal velocity. The Ca near the star is doubly ionized. In the early M stars the Ca does not recombine to Ca II until the terminal velocity has been reached, but in the later stars, the Ca II extends into regions where the matter is still being accelerated. A further study of the gas shells of M stars was conducted by Reimers (1975) for a larger sample of stars. His work verified the increase of H4 and K4 to later spectral type and the correlation of stronger K4 width with lower measured velocity (or position of line center). In addition, Reimers observed variability in the K line profiles of some of the earliest M giants in the sense that a single star shows the width-velocity correlation: while the blue edge of the profile remains roughly stationary, the position of the red edge varies with time. Reimers interpreted these

* Visiting Astronomer, Cerro Tololo Inter-American Observatory, supported by the National Science Foundation under contract No. AST 74–04128.

observations as supporting Deutsch's model that the variation of the K4 profile with spectral type is due to ionization effects and velocity gradients.

The most readily visible CS feature is the shell component of the Ca II reversal of the resonance lines at λλ3933 and 3968 (Deutsch 1960). The strong resonance lines of Na I at λλ5890 and 5896 show asymmetric blue-displaced cores in some M giants. In addition, Hα is seen to have asymmetric cores in many M stars. Thus there are three strong, easily observed features which arise in quite different conditions: resonance lines of a neutral atom, resonance lines of an ionized atom, and an excited line from the most abundant element. We have accumulated data in a large homogeneous sample of M giants in order to investigate the variation of the properties of CS shells as a function of spectral type or evolutionary phase. We combine this with some observations of the resonance line of Sr II at λ4077 and some infrared observations of the 10 μm silicate feature. The stars in the sample are fainter than $M_v = -2.5$, where the absolute magnitudes are derived primarily from the Ca II emission width determinations by Wilson (1976).

II. OBSERVATIONS

Observational material for this project was obtained at several different telescopes and spectrographs. The spectrograms of the Ca II H and K lines were taken primarily by Dr. Armin J. Deutsch with the coudé spectrograph of the 5 m reflector.[1] This collection was supplemented by plates obtained by O. C. Wilson and by A. M. B. at the 100 inch (2.5 m) Mount Wilson telescope and by plates from the Hale Observatories' plate file. This set of 42 spectrograms has a reciprocal dispersion of 10 Å mm^{-1}, except for the following 12 stars which were observed with the 5 m telescope at 4.5 Å mm^{-1}: β And, α Cet, ρ Per, μ Gem, λ Dra, δ Vir, σ Lib, κ Ser, δ Oph, R Lyr, λ Agr, and β Peg. In addition, spectrograms of 2 Cen, δ^1 Aps, and HR 7682 were obtained at Cerro Tololo by W. H. at 9 Å mm^{-1}, and echellograms at 5.1 Å mm^{-1} of X Her and HD 207076 taken by W. H. at Kitt Peak for another purpose were used. Information on the CS component of the Sr II line at 4077 Å was also obtained from the spectra of the latter five stars. All these spectrograms were intentionally heavily exposed to reveal the deep cores of the Ca II features.

Most of the spectrograms of the region covering the Na D lines and Hα were obtained at the coudé spectrograph of the Lick 3 m telescope at a reciprocal dispersion of 8 Å mm^{-1}. The details of those spectrograms and the particular stars are listed by Merchant (1967). The other coudé spectrograms were obtained by Deutsch with the 5 m telescope; they have a reciprocal dispersion of 6.7 Å mm^{-1}. Most of these spectra are on IIa-D emulsion and are heavily exposed to reveal the CS cores. Plates at Hα on IIa-F emulsion were available for some of the stars observed by Deutsch at the D lines.

All the plates have photometric calibrations. The Lick and Mount Wilson plates have strips of known intensity impressed on the plate during the stellar exposure. The Palomar spectra were developed simultaneously with a plate from an auxiliary calibration spectrograph which uses a wedge-shaped opening. Calibration plates were obtained with a spot sensitometer and developed simultaneously with the spectrograms taken at Kitt Peak and Cerro Tololo.

Figure 1 (Plate 3) shows a reproduction of the spectra of some representative M giants in the region of the Ca II K line from the Palomar spectrograms. The Ca II CS component is a sharp, deep, blue-shifted absorption core (K4) superposed on the chromospheric K2 emission component. The figure shows clearly the increasing strength or breadth of the CS component with advancing spectral type. It also shows the change in position of the centroid of the line, or, more particularly, the red edge of the line. Figure 2 (*left panel*) shows intensity tracings of a sample of the Lick spectra at the Na I line at 5890 Å. The asymmetric D line profile results from the superposition of a P Cygni shell line profile on the deep photospheric absorption feature. The asymmetry becomes

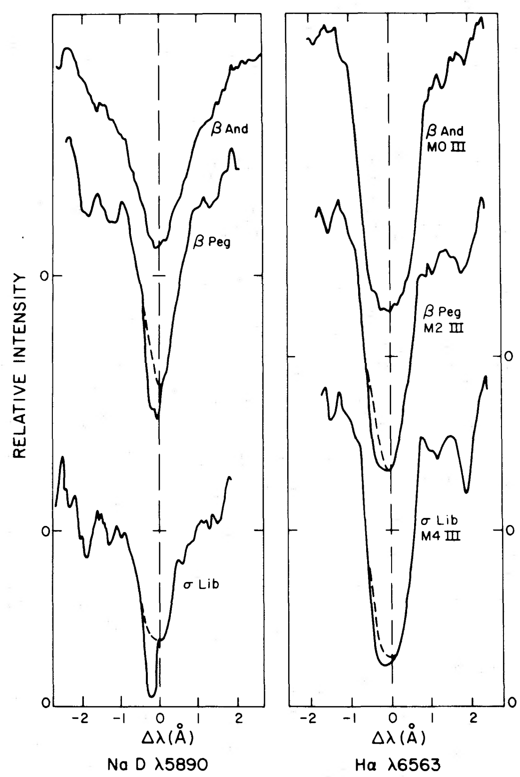

FIG. 2.—Microphotometer tracings of the Na I λ5890 line (*left panel*) and Hα (*right panel*) in representative M giants. The dotted lines outline the "effective continuum" used in the measurement of the CS Na line strength.

[1] Dr. Deutsch and A. M. B. had begun a collaborative project on the CS shells of M giants, but the research was interrupted by Deutsch's death in 1969. The spectroscopic material and notes have kindly been made available to the authors by the Director of the Hale Observatories.

increasingly apparent and occurs in a greater fraction of the stars as one looks in cooler stars. Figure 2 (*right panel*) shows the Hα line in the same three stars. This feature appears to be asymmetric in about half the stars in our sample.

In addition, infrared observations were made of several M giants to look for CS dust via the 10 μm silicate feature. Data on X Her and HD 207076 are taken from Hagen (1978); the other stars were observed at Cerro Tololo using the 1.5 m telescope with a germanium-doped bolometer. The 8–13 μm region was observed with a series of six filters of 1–2 μm bandwidths, and magnitudes at 2.2, 3.5, and 4.8 μm were measured.

III. LINE STRENGTHS AND VELOCITY DISPLACEMENTS OF CS FEATURES

Line strengths and positions were measured for the CS features in all the stars in which they appeared.[1] Most of the measurements of the K line were by Deutsch. He tabulated the width of the K4 core, which is a good indicator of the strength because the central intensity is essentially zero and the sides of the lines are very steep. (Following Deutsch [1960] we have ignored the contribution of the chromospheric K3 absorption component. As partial justification, we point out that in the M0 giants, where no CS component is seen, the K3 component is very weak; see the reproduction of the spectrum of α Lyn in Fig. 1.) The positions were measured on a standard measuring engine relative to the photospheric lines (excitation potential greater than 1 eV in order to avoid errors due to unresolved CS components) and the comparison lines. The K4 width and central velocity were measured for the CTIO plates using a Grant measuring engine. No velocities are quoted for the stars observed with the KPNO echelle because of the difficulty of measuring the absolute line position from the microphotometer tracings; however, the line width could be measured reasonably accurately. Table 1 presents all the stars observed grouped by spectral type and gives the K4 line widths in mÅ and the displacement from line center in km s^{-1} in columns (2) and (3).

For the D lines and Hα, the position of the deepest part of the line core was measured on a Grant measuring engine. The stellar velocity was determined from the positions of 10–20 photospheric lines. The displacement of the CS core is the difference in those velocities. The position of line minimum was also measured for most of those lines which appear to be completely symmetric. Those measurements give an estimate of the error of the displacement of the strong photospheric line compared to the weak photospheric lines used to find the stellar radial velocity; 75% of those "displacements" are between -2 and $+1$ km s^{-1} and 95% between -3 and $+3$ km s^{-1}. The core displacement from line center is given in Table 1 for the D lines in column (5) and for Hα in column (7).

A measure of the strength of the CS part of the line was made. The red side of the line profile was reflected around the line-center position and superposed on the blue side following Weymann (1962) and Hagen (1978). The asymmetric portion could thus be isolated and measured. These measurements approximate the true equivalent width of the CS P Cygni profile (absorption plus emission) and are easier to do with consistency over the large sample of stars. The D lines are thought to be formed in the CS shell, and the atoms see a "continuum" that is the edge of the photospheric line rather than the stellar continuum; the equivalent widths were measured with respect to this "effective continuum." For Hα, however, the asymmetry probably arises in the chromospheric layers. The main line-forming region for all parts of the line covers a smaller geometric distance, not out at a few stellar radii where the CS shell proper is. The equivalent widths for the Hα asymmetric features are referred to the stellar continuum in the region near Hα. These equivalent widths are in Table 1 in column (4) for Na (an average of the values for λλ5890 and 5896) and in column (6) for Hα.

The average line strengths and displacements for the CS features for each spectral type are given in Table 2. Figure 3 shows the run of equivalent width and velocities with spectral type for all three features. The Ca II K4 feature shows a very regular increase in strength toward late spectral types, while the measured line-center velocity decreases from -18 km s^{-1} to 11 km s^{-1}; this effect has been discussed by Deutsch (1960) and Reimers (1975). As is shown by the standard deviations of the mean given in Table 2, there is considerable scatter; some of this scatter is measurement uncertainty, but part of it is intrinsic variation in the physical extent of the shell from star to star. Circumstellar Na I begins to appear in giant stars of spectral type M2 and later and even then is visible in only 45% of the giants. The velocity of the Na I CS core appears to show a slight increase with decreasing stellar surface temperature. The average equivalent width for the CS Na I line for M giants is 230 ± 75 mÅ. An asymmetry is visible in the Hα line in stars of all spectral classes, in about 50% of the stars in our sample. Figure 3 shows that neither the strength of the core nor its position changes much with spectral type. (This is counter to a statement made by Reimers [1975] that the equivalent width of CS Hα increases from 20 to 100 mÅ; because he does not list his data, a meaningful evaluation cannot be made.) The average equivalent width is 27 ± 10 mÅ, and the average displacement is -3.8 ± 1.6 km s^{-1}. A larger sample of M0–M4 stars, which includes some supergiants (all those listed in Table 2 by Merchant 1967), shows that whenever CS cores are visible in the D lines, the Hα line is asymmetric. The average

[1] Contamination by interstellar (IS) components of Na I and Ca II was assumed to be negligible, except in ψ Vir, where the IS Na I lines are obvious. The stars in our sample are typically less than 100 pc distant, and the average IS Ca II K line is ~25 mÅ per 100 pc from Hobbs's (1978) data, while the CS features are several hundred mÅ. The IS line positions would have to be fortuitously located at -6 to -11 km s^{-1} to be confused with the CS Na I features in the 12 stars with asymmetric Na I lines.

TABLE 1

CIRCUMSTELLAR LINE STRENGTHS AND VELOCITIES

SPECTRAL TYPE AND NAME	HD (1)	Ca K W (mÅ) (2)	Ca K ΔV (km s⁻¹) (3)	Na D W (mÅ) (4)	Na D ΔV (km s⁻¹) (5)	Hα W (mÅ) (6)	Hα ΔV (km s⁻¹) (7)
M0 III:							
β And	6860	100	−24	sym	−2	sym	−3
γ Eri	25025	70	−21	sym	+0.5	20	−4
υ Gem	60522	0	...	...	...	...	...
α Lyn	80493	0	...	sym	−2	17	−6
μ UMa	89758	0	...	...	...	sym	0
75 Leo	98118	0:	...	...	...	...	...
λ Dra	100029	200	−15	sym	0	sym	0
106 Her	168720	0	...	sym	+4	sym	+3
α Vul	183439	75	−9	sym	+1	sym	−1
M1 III:							
υ Cet	12274	...	...	sym	+2	sym	+0.5
HR 881	18438	250	−16	...	...	...	...
HR 2275	44131	100	−26	sym	0	13	−0.4
HR 2822	58215	50:	−11	...	...	...	...
HR 3288	70652	...	...	sym	−0.3	sym	−1.5
HR 3820	83069	75	−23	sym	+0.5	29	−4
HR 3923	85951	100	−11	...	...	...	...
ν Vir	102212	200	−17	sym	−1.5	20	−4
3 CVn	107274	60	−23	...	...	...	...
κ Ser	141477	100	−18	...	...	...	...
δ Oph	146051	100	−13	sym	+1.5	sym	−2
24 Cap	200914	...	...	sym	+3	sym	−1.5
2 Peg	204724	...	...	sym	0	...	...
M2 III:							
χ Peg	1013	180	−16	sym	0	sym	−2
HR 363	7351	200	−22	sym	−5	...	...
α Cet	18884	250	−22	sym	+1	30	−4
π Leo	86663	50	−14	...	...	...	...
83 UMa	119228	200	−16	...	...	...	...
HR 5219	120933	180	−11	200	−8	40	−5
HR 6128	148349	150	−12	...	...	...	...
λ Aqr	216386	200	−16	sym	−0.5	25	−5
β Peg	217906	400	−12	200	−6	44	−4
φ Peg	223768	100	−15	...	...	...	...
M3 III:							
47 Psc	2411	400	−6	...	...	...	...
o^1 Ori	30959	...	...	270	−7	42	−4
HR 2018	39045	...	...	215	−9	50	−5
η Gem	42995	600	−25	cores?	−8	...	...
μ Gem	44478	300	−14	sym	−3	...	...
ψ Vir	112142	200	−14	Interstellar		20	−5
δ Vir	112300	200	−15	sym	−1	28	−3
η Sgr	167618	...	...	sym	0	sym	0
29 Cap	202369	...	...	sym	−1	sym	0
ψ Peg	224427	...	...	sym	+1	19	−5
M4 III:							
ρ Per	19058	500	−10	140	−9	...	...
54 Eri	29755	250	−21	...	...	...	...
4 Dra	108907	100	−14	...	...	...	...
HR 5299	123657	400	−5	...	...	...	...
σ Lib	133216	400	−12	200	−10	38	−4
δ^1 Aps	145366	400	−6	...	...	...	...
HR 8621	214665	325	−13	...	...	...	...
M5 III:							
HR 4184	92620	...	...	sym	−3	sym	−3
VY = 56 Leo	94705	500	−9	...	...	sym	0
RR UMi	132813	400	−21	...	...	...	...
R Lyr	175865	600	−8	250	−11	20	−6
M6 III:							
RZ = 45 Ari	18191	...	...	210	−10	≤10	...
HR 1693	33664	...	...	sym	−3	...	...
ω Vir	101153	...	−12	250	...	...	...
2 Cen	120323	300	−13	...	...	...	...
τ^4 = 17 Ser	139216	...	...	350	−9	...	...
X Her	144205	700	...	...	...	...	...
g = 30 Her	148783	600	−8	240	−11	sym	0
M7 III:							
BD −02°5631	207076	600	...	...	...	...	...

TABLE 2

AVERAGE LINE STRENGTHS AND VELOCITIES WITH SPECTRAL TYPE

Spectral Class and Line	$\overline{W} \pm \sigma$ (mÅ)	$\overline{\Delta V} \pm \sigma$ (km s^{-1})	Frequency of Occurrence	Red Edge (km s^{-1})	Blue Edge (km s^{-1})
M0 III:					
Ca K	110 ± 60	−17 ± 7	4 of 9	−13	−21
Na D	0	...	0 of 6		
Hα	19 ± 2	−5 ± 1	2 of 7		
M1 III:					
Ca K	120 ± 70	−18 ± 5	9 of 9	−13.5	−22.5
Na D	0	...	0 of 8		
Hα	21 ± 8	−3 ± 2	3 of 6		
M2 III:					
Ca K	190 ± 90	−16 ± 4	10 of 10	−9	−23
Na D	200 ± 0	−7 ± 1	2 of 6		
Hα	35 ± 9	−5 ± 1	4 of 5		
M3 III:					
Ca K	340 ± 170	−15 ± 7	5 of 5	−2	−28
Na D	240 ± 40	−8 ± 1	2 of 8		
Hα	32 ± 14	−4 ± 1	5 of 7		
M4 III:					
Ca K	340 ± 130	−12 ± 5	7 of 7	+1	−25
Na D	170 ± 40	−10 ± 1	2 of 2		
Hα	38	−4	1 of 1		
M5 III:					
Ca K	500 ± 100	−13 ± 7	3 of 3	+6	−32
Na D	250	−11	1 of 1		
Hα	20	−6	1 of 1		
M6 III:					
Ca K	530 ± 210	−11 ± 3	3 of 3	+9	−31
Na D	260 ± 60	−10 ± 1	4 of 5		
Hα	≤ 10	...	1 of 2		
M7 III:					
Ca K	600	...	1 of 1	...	...

displacement velocities for both the D lines and Hα are always less than those for the K4 component of the Ca II lines.

Figure 4 shows the relationship between the K4 strength and the measured position of line center expressed as a velocity. The mean position for each spectral type is given, but there is considerable scatter from star to star. Apparently, the properties of the CS envelopes vary within a given spectral class; knowledge of the temperature and luminosity of the central star alone is not sufficient to determine the shell conditions. However, despite the scatter, the trend to wider, less blue-shifted K4 cores toward later spectral class is real, as found by Deutsch (1960). The average positions of the red and blue edges of the K4 core for each spectral type are given in Table 2. Note that the entire core is shifted blueward of the line center for the early M giants, and that the red edge

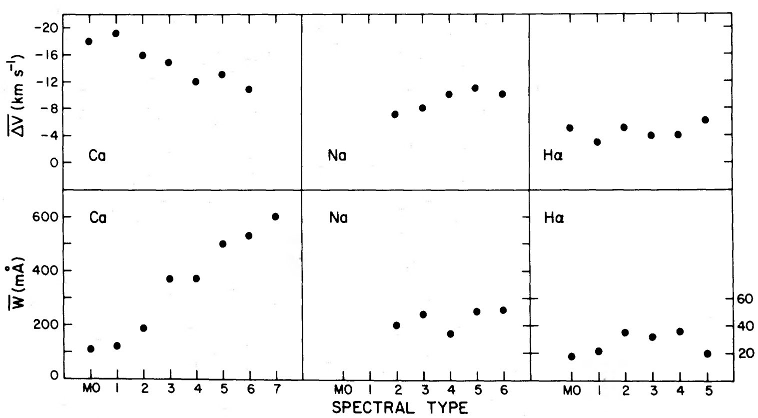

FIG. 3.—Average line strengths and velocities with spectral type

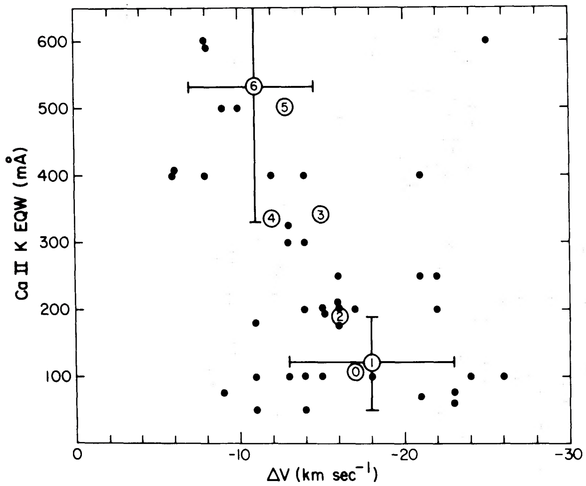

FIG. 4.—Ca II K4 strength versus measured line velocity. The filled circles represent individual stars, and the circled numbers the averages with spectral class. The point in the upper right is μ Gem. Possible reasons for its discrepancy are that it is a spectroscopic binary and also the brightest star in M_v (by $\sim$0.7 mag) included in the sample.

extends redward of line center for the late giants. As the line increases in width, the position of the red edge changes from -13 km s^{-1} at M0 to $+9$ km s^{-1} at M6—a total range of 22 km s^{-1}; this is to be compared to the broadening at the blue edge of only 10 km s^{-1}, from -21 km s^{-1} at M0 to -31 km s^{-1} at M6.

IV. ANALYSIS

The Kunasz-Hummer code for the formal solution of the equation of transfer in an expanding, extended atmosphere was used to interpret the observed line profiles (Kunasz and Hummer 1974). In the case of the Ca II lines, the shell was modeled as lying over a bright core with a chromospheric K2 emission profile. The results of interest, the positions of the red and blue edges of the K4 core, were not sensitive to the shape or intensity of the K2 emission. In the formal solution of the equation of transfer, it is necessary to specify the source function throughout the shell. Because of the extreme optical thickness of these lines, the position of the red and blue edges of K4 proved to be insensitive to the value of the source function, so long as the source function was low enough to produce the observed strong absorption cores. The value of the source function did affect the height of the K2 emission peaks and the small but nonzero residual intensity in the core; however, the scope of this research does not include interpreting these features. Line profiles were calculated for various shell parameters in order to determine those which most strongly affect the positions of the red and blue edges of the K4 core. As can be seen in the parametric analysis of shell lines in α Ori by Boesgaard (1979) and in the analysis of the formation of CS P Cygni profiles by Hagen (1978), the extent of the shell and the distribution of matter within it have little effect on the resultant profile. Parameters seen to affect the position of the line edges are turbulent velocity, optical depth, and velocity gradients. The exact functional dependence of velocity on distance from the central star is not important; the parameters of interest proved to be only the minimum (inner) and maximum (outer) velocities, for a velocity gradient increasing outward through the shell. In the calculations presented here, we have used a linear velocity law: $V = V_1 + V_2 r$.

Figure 5 shows the effect of optical depth and turbulent velocity on the K4 feature. The result, not particularly surprising for these extremely optically thick lines, is that turbulence is far more effective than the optical depth in broadening the line. In the past, most

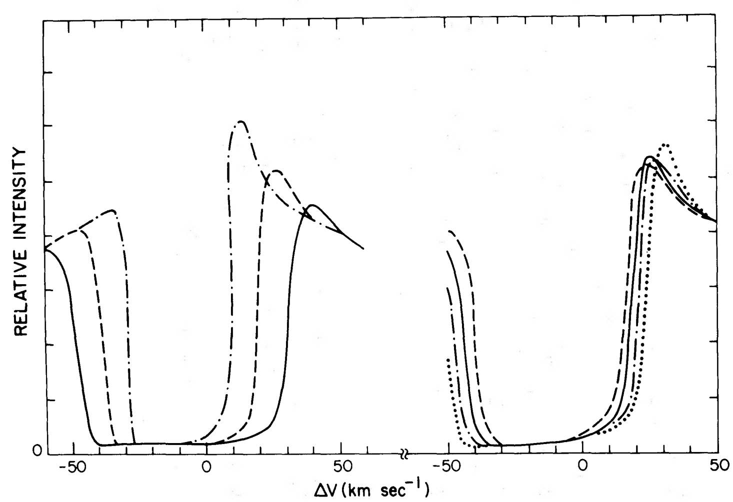

FIG. 5.—The effect of turbulence (*left*) and optical depth (*right*) on the K4 profile. Turbulent velocities (*left*) are: 5 (*dash-dotted line*), 10 (*dashed line*), and 15 km s^{-1} (*solid line*). Other shell parameters are a velocity gradient from 5–20 km s^{-1} and optical depths scaled from $\tau = 2000$ for $\xi = 5$ km s^{-1}. Optical depths (*right*) are: 100 (*dashed line*), 300 (*solid line*), 1000 (*dash-dotted line*), and 3000 (*dotted line*). Other shell parameters are a velocity gradient from 5–30 km s^{-1} and $\xi = 10$ km s^{-1}.

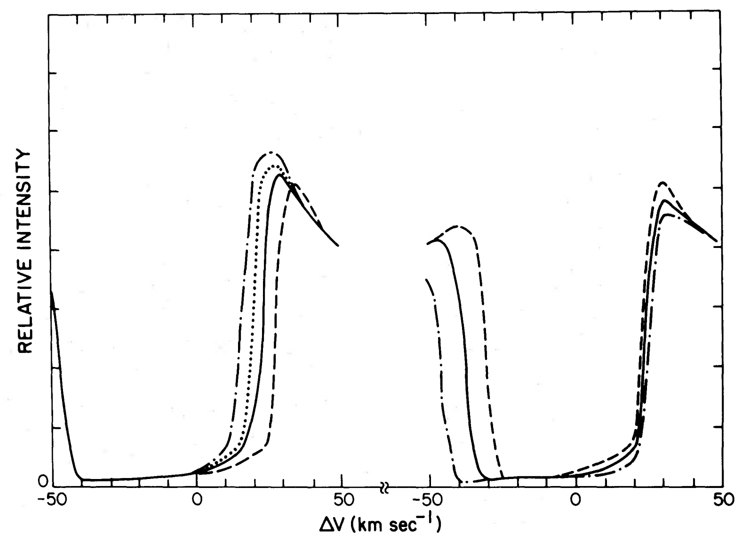

FIG. 6.—The effect of inner (*left*) and outer (*right*) shell velocity on the K4 profile. Inner shell velocities (*left*) are: 0 (*dashed line*), 2 (*solid line*), 5 (*dotted line*), and 10 km s^{-1} (*dash-dotted line*). Other shell parameters are: outer shell velocity 30 km s^{-1} and τ = 1000. Outer shell velocities (*right*) are 10 (*dashed line*), 20 (*solid line*), and 30 km s^{-1} (*dash-dotted line*). Other parameters are: inner shell velocity 0 km s^{-1} and τ = 1000.

mass-loss rates for M giants have been based on interpreting the width of the H and K lines in terms of the amount of CS material in the line of sight (Deutsch 1960). Because of the dominating influence of velocity on the line width, that interpretation and those mass-loss rates are unreliable.

In Figure 6 the effects of the inner and outer expansion velocities are shown. The inner (minimum) velocity affects the red edge of the profile only. The blue edge is affected by the outer (maximum) shell velocity which also exerts a small influence on the red edge.

A series of line-profile calculations was also performed in order to investigate the effect of velocity gradients on the measured intensity minima of the H and Na lines. For these optically thin lines, the radiative transfer in the shell is essentially a pure scattering process, and the source function arises from the photospheric mean intensity diluted outward through the shell. In the calculations of the line profiles, the source function was assumed to vary as (radius)$^{-2}$ throughout a shell overlying a bright core with a strong Gaussian absorption profile. The constant of proportionality in the source function was chosen such that net shell absorption equal net shell emission, a necessary condition for pure scattering as long as a negligible fraction of the shell is occulted by the central star. The line profiles were then smoothed to correspond to a dispersion of 8 Å mm^{-1}.

The position of line minimum can be used to measure the gas expansion velocity for a shell with constant expansion velocity (Hagen 1978). However, in the presence of velocity gradients, the situation is more complicated. Increasing both the inner (minimum) and outer (maximum) shell expansion velocities resulted in an increase in the displacement of line minimum, as seen in Figure 7. The situation is further complicated because the displacement of line minimum increases for stronger lines; because of the greater optical depth, the formation of the line profile is dominated by regions farther out in the shell at greater expansion velocities. Since several variables affect the position of line-core displacement, the measured Hα and D line velocities cannot be used to specify velocity gradients.

However, the measured Hα and D line velocities can be explained qualitatively as resulting from the formation of lines of moderate optical thickness in an envelope with a velocity gradient. Inasmuch as the optical depths in the Hα and D lines are lower than in H and K, the observed line profile will be dominated by the innermost, lowest velocity Na I and H I. As seen in Hagen (1978), the displacement of line minimum is decreased for weak lines. The low degree of asymmetry observed for the Hα lines indicates that their particularly low measured velocities arise at least in part from this effect. At present the relative contributions to the lowering of the measured velocities for the Hα and D lines of line formation in a velocity gradient and lower optical depth cannot be separated.

We have not attempted to derive detailed models for the velocity structure of M giant CS envelopes since the effects of velocity gradients, turbulence, and optical depth are not clearly separable. However, certain assumptions can reduce the number of free parameters. Observations of the CS component of the Sr II line at 4077 Å in some of the stars were used to derive probable shell optical depths for the Ca II K line through the assumptions of cosmic abundances and that the regions of Ca II and Sr II coincide in the envelope (as these two elements have similar ionization potentials). The optical depth of the Sr II λ4077 line was determined for the stars observed at Kitt

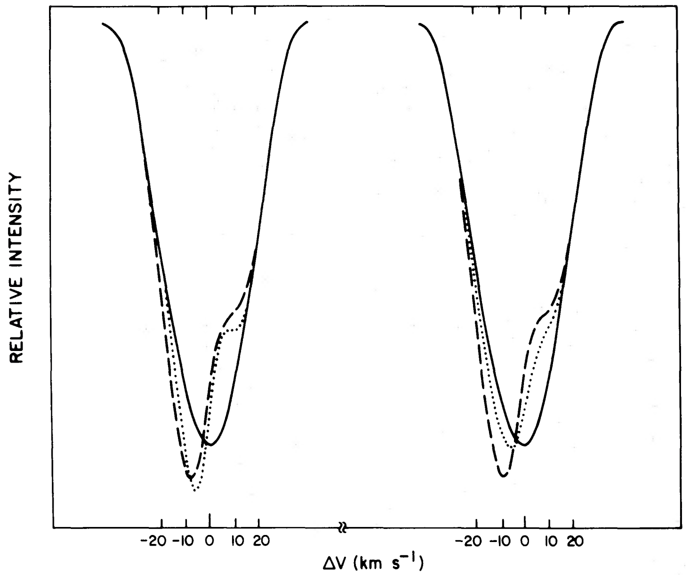

FIG. 7.—Variation of line core minimum with outer (*left*) and inner (*right*) shell velocity. Outer shell velocities (*left*) are: 10 (*dotted line*) and 20 km s^{-1} (*dashed line*). Note increased displacement of line core minimum for increasing outer shell velocity. Other model parameters are: inner shell velocity 5 km s^{-1} and $\tau = 3$. Inner shell velocities (*right*) are: 0 (*dotted line*) and 10 km s^{-1} (*dashed line*). Note increased displacement of line core minimum for increasing inner shell velocity. Other model parameters are: outer shell velocity 20 km s^{-1} and $\tau = 3$. The solid lines represent the underlying photospheric profile.

Peak and Cerro Tololo from the degree of asymmetry in the observed line profile following Hagen (1978). (This part of the analysis assumed a constant expansion velocity of 10 km s^{-1}.) The probable values for τ(Ca II) are given in Table 3 for those stars for which we have observations of the Sr II line. We can now assume an upper limit on τ(Ca II) of about 400 for the early M giants, with τ(Ca II) increasing to 1000 by M7. These values of τ were used in the calculation of the model Ca II line profiles. As optical depth is defined to be inversely proportional to turbulent velocity, for a given run of profile calculations of varying turbulence, the optical depth was scaled so that the number of particles in the line of sight remain constant. The Ca II optical depths quoted in Table 3 refer to a turbulence of 5 km s^{-1}.

Some additional information on the velocity structure in the shell can be obtained from measurements of the ratio of the CS strengths of the two Na D lines and application of Strömgren's (1948) calculations for interstellar gas. If the absorbing atoms follow a Gaussian velocity distribution, the Doppler velocity can be derived from the doublet ration D2/D1 and the equivalent width of D1. Although it is difficult to make accurate measurements of the CS component of D lines, we have usable data for 8 stars of spectral types M2–M6. With the assumption that the conditions in circumstellar shells are not vastly different from those in the interstellar gas, we can find values of the Doppler parameter $b(\lambda)$ from Strömgren's Table 2. The shell turbulent velocities derived in this manner are typically 3–4 km s^{-1}.

TABLE 3

ESTIMATED Ca II K AND DUST OPTICAL DEPTHS; MASS-LOSS RATES

Star	Spectral Type	τ (Sr II 4077)	τ (Ca II K)	τ (10 μm)*	*ML* Rate ($M_\odot$ yr^{-1})
HR 7682	M3 III	< 0.3	< 400	...	...
δ^1 Aps	M4 III	0.3	400	< 0.02	8×10^{-10}–3×10^{-9}
HR 587	M5 III	...	...	0.06	$>6 \times 10^{-9}$
X Her	M6 III	0.5	600	0.1	1.2×10^{-8}
ϵ Oct	M6 III	...	...	0.06	$>6 \times 10^{-9}$
2 Cen	M6 III	< 0.3	< 400	< 0.05	$<5 \times 10^{-9}$
δ^2 Gru	M6 III	...	...	0.02	2×10^{-9}
HD 207076	M7 III	0.9	1000	0.2	2.2×10^{-8}
HR 5134	M7 III	...	...	0.05	$>5 \times 10^{-9}$
R Dor	M7 III	...	...	0.06	$>6 \times 10^{-9}$

* Assume dust begins at 1 R^* and is distributed proportional to (radius)$^{-1.5}$.

V. DISCUSSION

a) Early M Giants

The observation of greatest interest for the early M giants is the position and narrowness of the observed K4 cores. There is no evidence for Ca II at zero velocity (see Fig. 4). Profiles were calculated for the early M giants both for constant expansion velocity and velocity gradients. If the profiles of the M0–M1 giants are interpreted as being formed in a region of constant expansion velocity, the shell turbulence is on the order of 2 km s^{-1}. If the profile is formed over a velocity gradient, the turbulence would have to be even less; however, as the observed profiles are very narrow (< 10 km s^{-1}), we cannot be observing Ca II over a large velocity gradient.

None of the M0–M1 giants show CS cores for Na I but both CS Ca II and Na I features are present on Mauna Kea coudé spectra at 6.7 Å mm^{-1} for the supergiants λ Vel (K5 Ib) and σ CMa (M0 Iab), and the Na I cores are of sufficient strength to allow a velocity determination. The measured velocities for CS Na I and Ca II agree with each other in both stars and show no evidence for zero-velocity Ca II or Na I. This supports the picture that no low stages of ionization (Ca II, Na I) are present in the shell at zero expansion velocity. These results indicate that the mechanism of mass loss must turn on so rapidly that no significant amount of Ca II can be found at velocities less than the terminal velocity, or that the mechanism acts upon calcium which has been doubly ionized in the chromosphere and which does not recombine until terminal velocity has been reached.

By spectral type M2, CS cores are observed in some stars for the Na D lines. The measured core positions give lower velocities than K4, due to velocity gradients and/or lower optical depth, as explained previously.

b) Late M Stars

According to the calculated profiles, if the observed K4 feature for an M4 star were formed at a constant expansion velocity, a turbulent velocity ξ of 5 km s^{-1} would be necessary to explain the observed line width. However, if the actual turbulent velocity in the shell is less, we must be observing CS Ca II over a velocity gradient. Although the available data are not sufficient to separate the effects of turbulence and velocity gradients, for a given value of ξ, the velocity gradient necessary to reproduce an observed profile can be determined. Table 4 gives possible combinations of shell turbulence and velocity gradients which reproduce the average observed profile for an M6 giant. The maximum possible ξ, 8 km s^{-1}, occurs for constant expansion velocity. As ξ decreases, Ca II in the shell must be observed over a greater range in velocity. The assumption of no net infall can be used to set a lower limit on ξ in the later giants, as the red edge of the K4 core lies at positive velocities. The turbulent velocity for an M6 giant must be at least 4 km s^{-1}.

As discussed in the previous section the doublet ratio for the CS Na D lines can be measured and used to estimate a Doppler parameter near 3–4 km s^{-1} in the shells. There is not sufficient data to investigate trends with spectral type. However, the ξ of 3–4 km s^{-1}, derived from the Na doublet ratio method for the late M stars, suggests that a velocity gradient rather than a large turbulence is probably responsible for the majority of the K4 broadening.

Information on the trend of ξ with luminosity is available from 6.7 Å mm^{-1} spectrograms obtained at Mauna Kea Observatory of α Ori (M2 Iab) and μ Cep (M2 Ia). Whereas ξ in M2–M3 giants must be on the order of 3 km s^{-1} or less, the K4 profiles indicate that the α Ori shell must have a turbulent velocity of at least 10 km s^{-1} and that of μ Cep at least 15 km s^{-1}.

c) Velocity Structure

The observed K4 line profile shows that the breadth and positions of the absorption change with spectral type. The calculated K4 profiles reveal that these changes result from an increase in the turbulence and line formation over a gradient in velocity. It is possible to derive limits on the turbulence in the shell by comparison of the observed and calculated profiles. Table 5 shows these limits as a function of spectral class. These limits are calculated for an envelope in which there is no velocity gradient. A variation in ξ with spectral type is clear; for the M0 giants, ξ must be the order of 2 km s^{-1} or less while for M6 giants ξ must be 4 km s^{-1} or more.

Figure 8 shows very schematic velocity curves for the CS shells of successively cooler M giants. The Ca II region moves in closer to the stellar surface for cooler stars so that the line is formed over a larger range of velocities. The turbulent velocity increases in the shells of the cooler stars. The turbulence found from the Na D lines indicates that there could be a gradient in the turbulent velocities also in the sense

TABLE 4

POSSIBLE COMBINATIONS OF TURBULENCE AND VELOCITY GRADIENTS TO FIT OBSERVED M6 PROFILE

ξ (km s^{-1})	V (km s^{-1})
8	11
6	4–19
4	0–23

TABLE 5

LIMITS ON SHELL TURBULENT VELOCITIES

Spectral Type	ξ (km s^{-1})
M0	≤ 2
M2	≤ 3
M4	≤ 5
M6	4–8

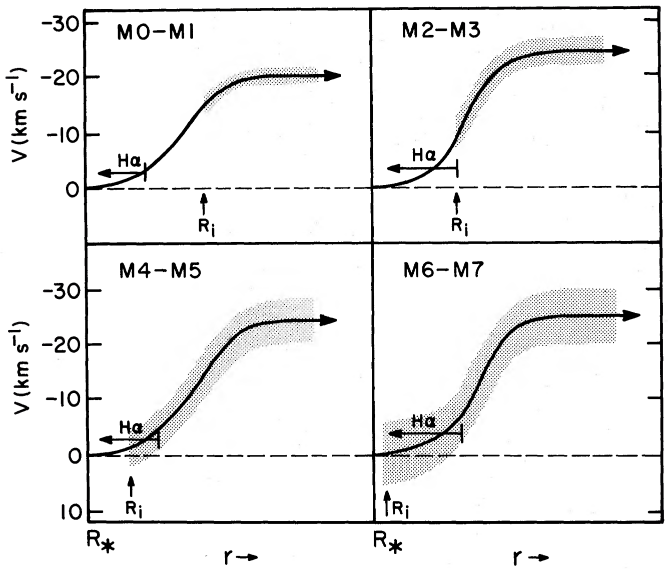

FIG. 8.—Schematic velocity curves for the envelopes of M giants. The velocity in the shell increases with distance r from the star as schematically illustrated by the solid line. The turbulence is shown by the cross-hatching, which shows the region over which the Ca II K4 feature is formed in the shell. The formation region for Hα is indicated by the arrows. The symbol R_i marks the inner boundary of the Ca II shell.

that the inner shell regions might have 1–2 km s^{-1} greater turbulence than the outer shell for the middle M-type giants.

d) *CS Dust*

Observations of the 10 μm silicate features of several M giants were used to study CS dust. No silicate feature was seen for δ^1 Aps (M4 III), ψ Phe (M4 III) ε Mus (M5 III), 2 Cen (M6 III), and HR 7625 (M6 III). Dust optical depths τ (10 μm), as determined following Hagen (1978) for several other M giants, are given in Table 3.

The mass-loss rates given in Table 3 were calculated assuming equal fractional condensations of Sr and Si as in Hagen (1978). These mass-loss rates must be taken as lower limits because of the uncertainties in the inner shell radii. At present, the upper limits for mass-loss rates based on the absence of a 10 μm silicate feature are considerably higher than those based on lack of asymmetry in the Sr II λ4077 line. The earlier M giants are not likely to have much CS dust and higher-resolution observations of the Sr II line should allow determinations of mass-loss rates for these stars.

e) *Mass-Loss Mechanism*

The presence of asymmetry in Hα in some stars of all spectral types M0–M5 III indicates that expansion is occurring in the chromospheric regions. Furthermore, Wilson (1960) has shown that the chromospheric K2 and H2 components are displaced to the blue in a sample of 44 mostly M-type stars and interprets this to mean that the chromosphere appears to expand at one-third to one-half the final envelope velocity. Reimers (1975) has reached a similar conclusion. This has implications regarding the mechanism of mass loss since radiation pressure on dust grains is a potent contender as the dominant cause of mass loss. However, silicate dust would not be expected to form at chromospheric temperatures (Fix and Alexander 1974). In fact, presence of a sufficient amount of dust can quench a chromosphere (Jennings 1973). Once grains form, radiation pressure on them will carry mass away, but apparently an additional physical process must operate in the hotter M giants—where no dust is expected or observed—to drive the mass loss.

Mullan (1978) has investigated supersonic stellar winds as a cause for mass loss in cool stars. He points out that if the sonic point of a stellar wind is below the altitude to which spicules can penetrate, a tremendous increase in the mass lost by a stellar wind will be seen (roughly a factor of 50), and expansion effects will be visible in the chromosphere. This mechanism for mass loss is consistent with the picture of M giant envelopes seen here with the expansion beginning in the chromosphere, and seen in K2, H2, and the Hα asymmetry. In the shells of the earliest M giants, Ca II is observable in absorption after the terminal expansion velocity has been reached. In the latest M giants, there is a significant amount of Ca II present in the shell near zero velocity. It is perhaps significant that CS dust becomes evident at roughly the same spectral type, ~M6 III, as does the possibility of observing Ca II at zero velocity. Perhaps it is only for these stars that sufficient cool material exists at densities high enough to allow significant grain formation before the onset of a supersonic wind.

VI. CONCLUSIONS

From this study of the average CS envelopes of M giants of types M0–M7, we have been able to deduce information about the velocity structure in the envelopes and about the mass loss mechanism.

The positions of the red and blue edges of the CS Ca II K4 profile were used to derive information on shell turbulent velocity, ξ, and velocity gradients within the envelopes. The narrow, entirely blue-shifted K4 cores for the earliest M giants cannot have been formed over a substantial velocity gradient. That no Ca II is seen at zero velocity indicates that the acceleration to a terminal velocity occurs extremely rapidly or that the mass-loss mechanism acts upon Ca III, which recombines only after the terminal velocity has been reached. The K4 feature broadens to later spectral type, due to an increase in ξ and/or the formation of the line profile over a velocity gradient. The turbulence in the shells of the M0 giants must be less than 2 km s^{-1} and increase to a value of at least 4 km s^{-1} for the M6 giants. The broadening of the K4 profile must be due at least in part to the increase of turbulence toward later spectral type. The D lines imply a value of the turbulence of about 3–4 km s^{-1} for the shells of the middle and late M giants.

Observations of circumstellar Hα in stars of all spectral classes M0–M6 III and systematic blue shifts of the chromospheric H2 and K2 features (Wilson 1960) indicate that the shell expansion begins well within the chromosphere. As grains are not likely to survive under chromospheric conditions, the mechanism for mass loss is probably not radiation pressure on grains, but could be supersonic winds such as those discussed by Mullan (1978).

Our analysis of the line profiles clearly shows that turbulence and velocity gradients are far more important in the broadening of the K4 feature than is the line optical depth. Consequently, mass-loss rates based on observations of these lines should be considered unreliable.

We are deeply indebted to the late Dr. Armin J. Deutsch with whom this research was begun. A. M. B. has benefitted from stimulating discussions with him about circumstellar shells; his plate material, velocity and line strength measurements, and extensive notes have been of inestimable value. We are grateful to Dr. Olin C. Wilson for many conversations and for the use of his spectrograms of the Ca II H and K regions. A. M. B. wishes to gratefully acknowledge the hospitality of the Hale Observatories and Director Horace W. Babcock during 1974, when part of this work was carried out. We also thank Miss Louise Lowen who measured many of Deutsch's spectrograms and assisted A. M. B. with his papers and plate collection. Due to the kindness of Dr. D. G. Hummer and Dr. Paul B. Kunasz, whose computer code we have used, the interpretation of the lines profiles has been greatly enhanced. W. H. would like to acknowledge the support of a Joseph A. Skinner fellowship from Mount Holyoke College. This research has been supported by NSF grants AST 73-04840 and AST 76-81608.

REFERENCES

Boesgaard, A. M. 1979, *Ap. J.*, **232**, in press.
Deutsch, A. J. 1960, in *Stellar Atmospheres*, ed. J. L. Greenstein (Chicago: University of Chicago Press).
Fix, J. D., and Alexander, D. R. 1974, *Ap. J.* (*Letters*), **188**, L91.
Hagen, W. 1978, *Ap. J. Suppl.*, **38**, 1.
Hobbs, L. 1978, *Ap. J. Suppl.*, **38**, 129.
Jennings, M. C. 1973, *Ap. J.*, **185**, 197.
Kunasz, P. B., and Hummer, D. G. 1974, *M.N.R.A.S.*, **166**, 57.
Merchant, A. E. 1967, *Ap. J.*, **147**, 587.
Mullan, D. J. 1978, *Ap. J.*, **226**, 151.
Reimers, D. 1975, *Mém. Soc. Roy. Sci. Liège*, 6e Sèr., **8**, 369.
Strömgren, B. 1948, *Ap. J.*, **108**, 242.
Weymann, R. J. 1962, *Ap. J.*, **136**, 844.
Wilson, O. C. 1960, *Ap. J.*, **132**, 136.
———. 1976, *Ap. J.*, **205**, 823.

ANN MERCHANT BOESGAARD: Institute for Astronomy, 2680 Woodlawn Drive, Honolulu, HI 96822

WENDY HAGEN: Center for Astrophysics, 60 Garden Street, Cambridge, MA 02138

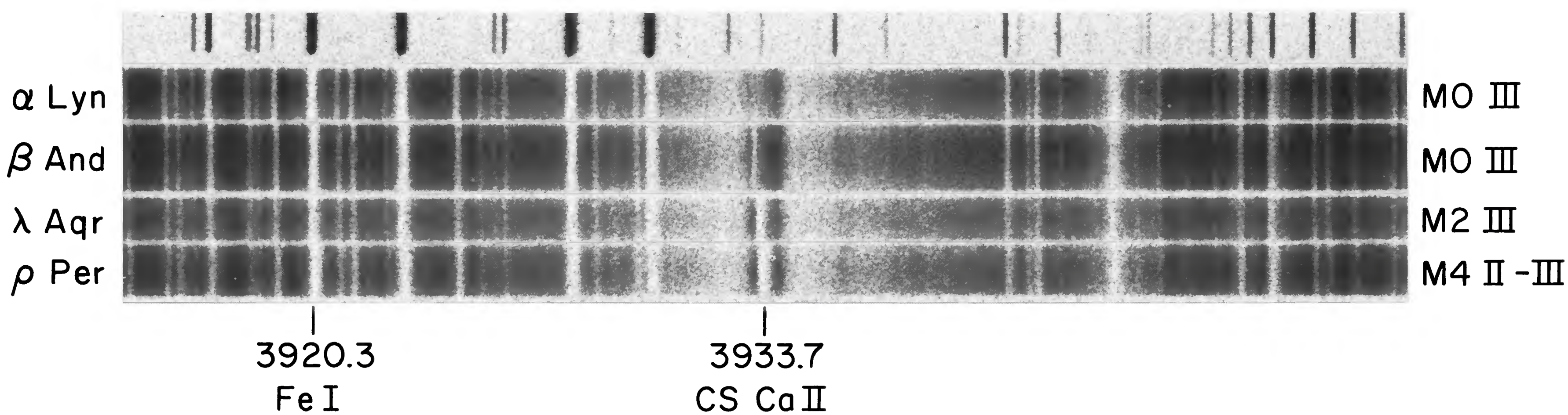

FIG. 1.—Representative spectra of the CS Ca II K4 feature in M giants. Note the widening of the feature toward later spectral type, with the blue edge of the core remaining relatively stationary while the red edge moves longward. The top spectrum, α Lyn, shows only the chromospheric Ca II K3 absorption.

BOESGAARD AND HAGEN (*see* page 129)